

## Comparison the effect of co-precipitation and sol-gel techniques on the structural and magnetic attributes of ZnO and Zn<sub>(1-x)</sub>Fe<sub>0.05</sub>Co<sub>x</sub>O nanoparticles for attaining room temperature ferromagnetism (RTFM)

S. Kanwal<sup>a,†</sup>, M. T. Khan<sup>a,†</sup>, A. Zaman<sup>a,\*</sup>, V. Tirth<sup>b,c</sup>, A. Algahtani<sup>b,c</sup>,  
T. Al-Mughanam<sup>d</sup>

<sup>a</sup>Department of Physics, Riphah International University, Islamabad 44000,  
Pakistan

<sup>b</sup>Mechanical Engineering Department, College of Engineering, King Khalid  
University, Abha 61421, Asir, Kingdom of Saudi Arabia

<sup>c</sup>Research Center for Advanced Materials Science (RCAMS), King Khalid  
University, Guraiger, P.O. Box 9004, Abha-61413, Asir, Kingdom of Saudi Arabia

<sup>d</sup>Department of Mechanical Engineering, College of Engineering, King Faisal  
University, P. O. Box 380, Al-Ahsa 31982, Kingdom of Saudi Arabia.

In current study, ZnO and Fe/Co co-doped ZnO (Zn<sub>1-x</sub>Fe<sub>0.05</sub>Co<sub>x</sub>O where x = 0, 0.005) nanoparticles were prepared by using two different methodologies: sol gel method and co-precipitation method. The structural properties were determined by X-Ray diffraction technique which verifies the hexagonal wurtzite structure of prepared nanoparticles. Crystallite size varies from 18.68-37.43 nm for the samples synthesized by co-precipitation method and it varies from 19.97-38.45 nm for sol-gel method. Fourier transform infrared transmittance spectra were used to investigate the type of functional groups present in all the prepared nanoparticles. The UV-Visible absorption spectroscopy was employed to investigate the optical properties of ZnO and doping of Fe/Co in ZnO semiconducting host. The energy band gap varies from 3.03 - 3.68 eV for the samples synthesized by co-precipitation method and for sol-gel method, it ranges from 3.13 - 3.86 eV, by increasing dopant concentration. Vibrating sample magnetometer was used to inquire the magnetic behavior of synthesized nanoparticles which shows the weak ferromagnetic behavior of the doped nanoparticles prepared by both the techniques. Samples prepared by co-precipitation method showed higher values of saturation magnetization and coercivity as compared to the samples prepared by the sol-gel method. In comparison of two synthesis techniques, a slight change was observed in the particle size, energy band gap and magnetization values. The improved optical and magnetic behavior favors the co-precipitation method rather than sol gel method for obtaining room temperature ferromagnetism for practical applications in spintronics field.

(Received March 1, 2023; Accepted August 23, 2023)

**Keywords:** Transition-metal doped ZnO nanoparticles, Co-precipitation and sol-gel technique, Hexagonal wurtzite structure, Room temperature ferromagnetism, Spintronics

### 1. Introduction

Nanotechnology, which deals with the particles in the size range 1-100 nm and have high surface to volume ratio, is an expanding field in materials science [1]. Nanoparticles (NPs) are the basic ingredients for the formation of new species because of their extraordinary size dependent characteristics. They exhibit greatly manageable physical, optical, structural and magnetic properties depending upon their size [2]. In continuation to nanotechnology, spin-based electronics is an interesting field by increasing degree of freedom in nanostructures for technological applications.

---

\* Corresponding authors: zaman.abid87@gmail.com

† These authors contributed equally to this work

<https://doi.org/10.15251/DJNB.2023.183.1025>

Diluted magnetic semiconductors (DMSs) are representing linkage between charge-based semiconductors and spin-based magnetism [3,4]. Spin addition to the basic electronics increases its application hugely including faster operation, storage density and reduction in rate of energy consumption [5]. By using both the spin and charge of electrons we will be able to use the ability of processing of information and mass storage in the same system. Lower solubility of magnetic elements in compounds makes it difficult to make semiconductors magnetic. The control on both spin and charge of electrons can be advantageous in semiconductors which have room temperature ferromagnetism (RTFM) [6].

In order to achieve room temperature ferromagnetism, the use of oxide based semiconducting host given preference because they have a wide band gap i.e., transparent to visible light and can be densely doped with n type carrier [7]. Oxide based semiconductors also have capability to grow at low temperature that will help in restricting the sample in single phase. Even though, different NPs are presenting the potency in various fields of technology, but ZnO have achieved prime importance due to the numerous uses in transparent conducting oxide (TCO), solar panels, ultra-violet lasers, light modulators, piezoelectric devices and light emitting diode (LED) etc. [8,9].

ZnO is a transparent metal oxide having large exciton binding energy of 60 meV and direct band gap of  $\sim 3.4$  eV even at room temperature. Room temperature ferromagnetism is a desired property in spintronics which can be attained by the addition of impurities, either noble metals (e.g. *Pd, Ag, Pt* etc.) or transition metals (e.g. *Al, Cr, Mn, Fe, Ni, Cu, Co* etc.). Many researchers work on zinc oxide semiconductors doped with transition metals (*Mn, Fe, Co, Ni*) to achieve room temperature ferromagnetism [10-12]. Considerable work had been done on cobalt doped zinc oxides and iron doped zinc oxides as diluted magnetic semiconductors (DMS).

The work on comparison of the structural, anti-bacterial and photocatalytic properties of ZnO nanoparticles prepared by sol-gel and biosynthesis techniques has been done by Md Jahidul Haque et al. [13]. Elahe Darvishi et al. also worked on the comparison of the ZnO nanoparticles prepared by the green method (using *Juglans regia* L. leaf extract) and chemical method for the enhancement of its bactericidal applications [14]. Various researches proved the increased ferromagnetism by increasing doping concentration in iron doped ZnO nanoparticles [15,16].

M.L. Dinesha et al. used solution combustion method for synthesis of iron and cobalt co-doped zinc oxide nanoparticles and they successfully achieved RTFM [17]. D. Sharma, R. Jha et al. used co precipitation method for synthesis of iron and cobalt co doped zinc oxide nanoparticles. They reported that the RTFM achieved due to the oxygen vacancies and grain boundaries [18-20].

Although, the abovementioned literature is available on Fe and Co co-doped ZnO nanoparticles, but the study of co-doping of both the transition metals in ZnO is insufficient yet. Also, there is not even a single research paper available for the comparison of Fe and Co co-doped ZnO NPs synthesized by two different techniques.

Several synthesis techniques have been adopted for the formation of TM-doped ZnO nanoparticles, such as sol-gel method, co-precipitation method, auto-combustion method, hydrothermal process, solid-state reaction method and many others [21,22]. From all of these, we have used co-precipitation method and sol-gel method in which various variables like reaction time, reaction temperature and pH have significant impact on the characteristics of NP's shape and size.

The present research is focused on fabrication of ZnO and  $Zn_{(1-x)}Fe_{0.05}Co_xO$  ( $x = 0, 0.005$ ) nanoparticles by two methods. One is sol-gel method and the other one is co-precipitation method. A comparison of structural, optical and magnetic properties of the NPs synthesized by these two different methods is discussed here in detail.

## 2. Experimental details

### 2.1. Materials

All the raw materials including  $[Zn(NO_3)_2 \cdot 6H_2O]$  (Sigma – Aldrich),  $[Fe(NO_3)_2 \cdot 3H_2O]$  (Sigma – Aldrich),  $[Co(NO_3)_3 \cdot 6H_2O]$  (Sigma – Aldrich), sodium hydroxide, ethylene glycol, citric acid and ammonia were used as received without extra refining.

## 2.2. Synthesis of ZnO and Zn<sub>(1-x)</sub>Fe<sub>0.05</sub>Co<sub>x</sub>O nanoparticles by sol-gel method

ZnO and Zn<sub>(1-x)</sub>Fe<sub>0.05</sub>Co<sub>x</sub>O (x=0, 0.005) nanoparticles were synthesized by using sol gel method. Firstly, take the required amount of water (312 ml) in beaker and put the beaker on the hot plate. Then added the required amount of [Zn(NO<sub>3</sub>)<sub>2</sub>·6H<sub>2</sub>O] in the beaker and start stirring. After stirring of 25minutes, we added the required amount of [Fe(NO<sub>3</sub>)<sub>2</sub>·3H<sub>2</sub>O] into the beaker followed by constant stirring for more 20minutes to get better results. After that the required amount of [Co(NO<sub>3</sub>)<sub>3</sub>·6H<sub>2</sub>O] was added for x=0.005 sample. After stirring for few seconds, the required amount of citric acid (2.88 ml) and ethylene glycol (1.26 ml) were added as a catalyst. To maintain the pH between 9 and 10, some amount of ammonia was added. After maintaining the pH, the temperature was adjusted at 80°C for two hours.

After two hours, the temperature raised to 120°C and solution was changed to gel form. After some time, the gel started burning which assured that the sample was synthesized successfully. Then the sample was dried in oven at 80°C for 2 hours. After drying, the sample was ground to change it in to fine powder. After that the sample was annealed at 300°C for 3 hours in a box furnace under air. After annealing, the samples were ready for different characterizations. Three samples (ZnO, ZnFe<sub>0.05</sub>O and Zn<sub>0.995</sub>Fe<sub>0.05</sub>Co<sub>0.005</sub>O) were prepared by following the above procedure.

## 2.3. Synthesis of ZnO and Zn<sub>(1-x)</sub>Fe<sub>0.05</sub>Co<sub>x</sub>O nanoparticles by co-precipitation method

ZnO and Zn<sub>(1-x)</sub>Fe<sub>0.05</sub>Co<sub>x</sub>O (x=0, 0.005) nanoparticles were also synthesized by using co-precipitation method. Initially, a homogenous mixture was prepared by adding [Zn(NO<sub>3</sub>)<sub>2</sub>·6H<sub>2</sub>O], [Fe(NO<sub>3</sub>)<sub>2</sub>·3H<sub>2</sub>O] and [Co(NO<sub>3</sub>)<sub>3</sub>·6H<sub>2</sub>O] in distilled water. The solution was constantly stirred for 1 hour, then added NaOH solution to maintain its pH at 9-11. The stoichiometric amounts of all the chemicals were mixed with constant stirring for 2 hours until milky brown precipitates were formed.

The solution was filtered on the filter paper, then washed thoroughly for 3-5 times with deionized water and with ethanol. Resulting solution was again filtered followed by drying at 80°C for 2 hours in an oven. The sample was grounded into a fine powder and annealed at 300°C for 3 hours in a box furnace under air. Three samples (ZnO, ZnFe<sub>0.05</sub>O and Zn<sub>0.995</sub>Fe<sub>0.05</sub>Co<sub>0.005</sub>O) were synthesized by following this procedure.

## 2.4. Samples' recognitions

For the rest of the paper, the correspondence for all samples is given below.

Sample's formulation	Sample's marker
ZnO by sol-gel method	ZnO (sol-gel)
ZnO by co-precipitation method	ZnO (co-prec)
ZnFe <sub>0.05</sub> O by sol-gel method	ZnFeO (sol-gel)
ZnFe <sub>0.05</sub> O by co-precipitation method	ZnFeO (co-prec)
Zn <sub>0.995</sub> Fe <sub>0.05</sub> Co <sub>0.005</sub> O by sol-gel method	ZnFeCoO (sol-gel)
Zn <sub>0.995</sub> Fe <sub>0.05</sub> Co <sub>0.005</sub> O by co-precipitation method	ZnFeCoO (co-prec)

## 2.5. Characterization techniques

The structural properties of Co- and Cu-doped ZnO nanoparticles were scanned by using (X-Pert Philips) X-ray diffractometer by applying Cu – K $\alpha$  radiations ( $\lambda = 1.54 \text{ \AA}$ ) at 40kV and 30mA from  $2\theta = 20^\circ - 80^\circ$ . Fourier transform infrared (FTIR) spectroscopy employing (Shimadzu IR–Tracer 100) was evaluated in the region of 1400 – 200  $cm^{-1}$ , to explain the infrared spectrum of transmission. Ultraviolet-visible (UV – Vis) spectroscopy is employed to interpret optical behavior by using UV–Visible spectrometer (Model: lambda 35, Make: Perkin Elmer) at room temperature. Magnetic properties (M – H curves) were determined by the Superconducting quantum interference device (SQUID, Model MPMS-3 from Quantum Design Inc.) in State Key Laboratory for Mechanical Behavior of Materials, Xi'an Jiaotong University, China, at room temperature under an applied field of 10 kOe.

### 3. Results and discussions

#### 3.1. X-Ray diffraction

Fig.1 displays the XRD spectra of ZnO(co-prec), ZnO(sol-gel), ZnFeO(co-prec), ZnFeO(sol-gel), ZnFeCoO(co-prec) and ZnFeCoO(sol-gel) nanoparticles. Main diffraction peaks for (1 0 0), (0 0 2) and (1 0 1) planes confirmed the hexagonal wurtzite structure. For all samples, nine significant peaks are noticed, labelled as (1 0 0), (0 0 2), (1 0 1), (1 0 2), (1 1 0), (1 0 3), (2 0 0), (1 1 2) and (2 0 1) with maximum diffraction intensity at (1 0 1) lies between 35.8° to 37.6°.

The XRD peaks are shifted towards the smaller angle by co-dopant concentration of Co and Fe in pure ZnO. It is due to the difference of ionic radii of  $Zn^{2+}$  (0.60 Å),  $Co^{2+}$  (0.58 Å) and  $Fe^{3+}$  (0.67 Å). Average crystal size is determined by Debye Scherer's equation [23],

$$\text{Average crystal size } (D) = 0.9\lambda/\beta\cos\theta$$

where  $\lambda$  represents the wavelength of the incident radiation i.e 1.45 Å,  $\beta$  is the full width at half maximum (FWHM) of (101) peak and  $\theta$  is the Bragg's angle.

And the unit cell volume is computed by the following relation,

$$V = 0.866a^2c$$

where 'a' and 'c' are lattice constants and 'u' is the constant for wurtzite structure computed by the relation,

$$u = \left(\frac{a^2}{3c^2}\right) + 0.25$$

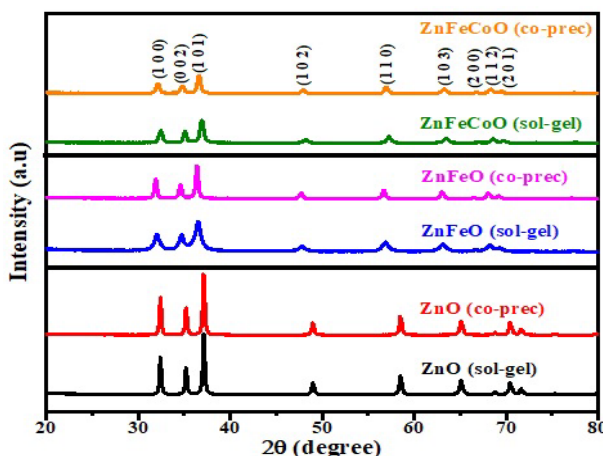


Fig. 1. XRD patterns of ZnO(co-prec), ZnO(sol-gel), ZnFeO(co-prec), ZnFeO(sol-gel), ZnFeCoO(co-prec) and ZnFeCoO(sol-gel) nanoparticles.

All the parameters of prepared samples are well match with the JCPDS card number 36-1451 [24]. Average crystalline size of ZnO sample synthesized by co-precipitation method is 37.43 nm and for sol-gel method, it is 38.45 nm. The average crystalline size for ZnFeO sample prepared by co-precipitation method is 18.68 nm and for the same sample synthesized by sol gel method have crystalline size of 19.97 nm. Also, for Co/Fe co doped sample synthesized by co-precipitation method, average crystallite size is 23.18 nm and the same sample synthesized by sol gel method have average crystalline size of 24.66 nm. This difference in the crystalline size may be due to the several times washing in co-precipitation method. As there are no extra peaks in the XRD pattern which confirm the formation of single phase for all samples.

Table 1 gives the values of lattice parameters ‘a’ and ‘c’ for most intense peaks. Lattice parameters are firstly decreased by the doping of Fe in ZnO and then, slightly increased by small amount of doping of cobalt which shows that the iron and cobalt atoms are well mixed with the zinc oxide atoms and do not change the structure of zinc oxide lattice which also confirms the hexagonal wurtzite structure of the prepared sample. It is also confirmed from the table that there is negligible variation in the lattice constant values of the samples synthesized by both techniques. As there is minor variation in radii of  $Zn^{2+}$  (0.60 Å) and  $Co^{2+}$  (0.58 Å), so the variation in the lattice constants of Co co-doped samples is not highly expected.

The values of unit cell volume ‘V’ are also written in Table 1. The unit cell volume of ZnO(co-prec) is  $47.60 (\text{Å})^3$  and of ZnO(sol-gel), it is  $47.57 (\text{Å})^3$ . For Co/Fe co-doped sample synthesized by co-precipitation method, the volume is  $34.36 (\text{Å})^3$  and for same sample synthesized by sol gel method has volume  $34.67 (\text{Å})^3$ . The unit cell volume of the sample ZnFeO prepared by co-precipitation method is  $32.93 (\text{Å})^3$  and for same sample prepared by sol gel method, the volume is  $33.98 (\text{Å})^3$ . The values of unit cell volume seconds the values expressed in the literature [25].

The variation in values of ‘a’, ‘c’ and ‘V’ by the doping of cobalt and iron is due to intra and inter nucleating forces in process of crystallization of ZnO with cobalt and iron ion concentration. Sharp peaks for all the samples in the spectrum proved the high crystallization. It is necessary to mention here that the crystalline character of wurtzite structure of ZnO is enhanced by the addition of Co as a co-dopant into the Fe-doped ZnO. Missing secondary phase related to magnetic precipitate unveiled the intrinsic ferromagnetic behavior [26]. A small difference in the values of all the parameters is observed for the sample synthesized by co-precipitation and sol-gel method, this difference is mainly due to several times washing of samples in co-precipitation method.

*Table 1. Lattice parameters  $a = b$  (Å),  $c$  (Å),  $2\theta$ , FWHM values,  $d$ -spacing, crystallite size and volume of ZnO (co-prec), ZnO (sol-gel), ZnFeO (co-prec), ZnFeO (sol-gel), ZnFeCoO (co-prec) and ZnFeCoO (sol-gel) by XRD profile.*

Sample Name	ZnFeCoO (co-prec)	ZnFeCoO (sol-gel)	ZnFeO (co-prec)	ZnFeO (sol-gel)	ZnO (co-prec)	ZnO (sol-gel)
$2\theta$ (degrees)	36.95	36.39	36.95	36.64	37.07	36.98
$d$ -spacing (Å)	2.43	2.47	2.42	2.45	2.49	2.50
FWHM (°)	0.45	0.42	0.59	0.54	0.35	0.33
Crystallite size (nm)	23.18	24.66	18.68	19.97	37.43	38.45
$a$ (Å)	2.84	2.85	2.80	2.83	3.24	3.72
$c$ (Å)	4.92	4.93	4.85	4.90	5.21	5.33
$V$ (Å) <sup>3</sup>	34.36	34.67	32.93	33.98	47.60	47.57

### 3.2. Fourier Transform Infrared Study

FTIR spectroscopy is a technique to investigate the elemental constituents and chemical bonding [27]. In present work, we have used the transmittance spectra of fourier transform infrared for analyzing different vibrational modes of the prepared sample. FTIR transmittance spectrum was observed in the wavelength range of 200-1400  $cm^{-1}$  (Fig.2). The iron doped zinc oxide samples synthesized by co-precipitation method shows transmittance peaks at 370, 510, 880 and 1385  $cm^{-1}$  and the same sample synthesized by sol gel method shows transmittance peaks at 370, 510, 868, 880 and 1385  $cm^{-1}$  as shown in figure. The iron and cobalt co-doped sample prepared by co precipitation method shows transmittance peaks at 370, 500, 868 and 1385  $cm^{-1}$  and the same sample prepared by sol gel method have transmittance peaks at 370, 670, 864 and 1385  $cm^{-1}$  as shown. The transmittance peaks from 370 to 510  $cm^{-1}$  are due to typical bond between zinc and oxygen and also due to the stretching vibrations of Zn-O bonds in octahedral positioning. Zn-O bonds in tetrahedral arrangement are so strong than the octahedral in prepared sample [28].

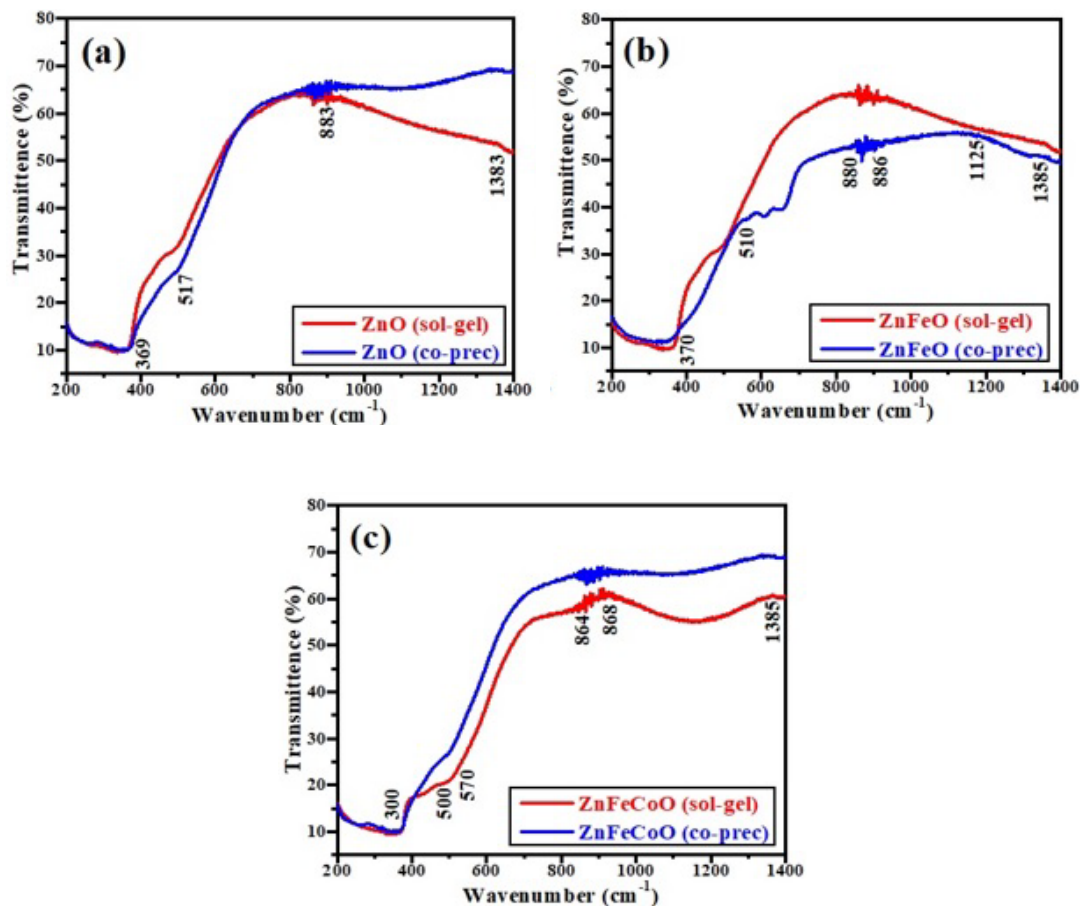


Fig. 2. FTIR spectra of (a) ZnO (co-prec) & ZnO (sol-gel) (b) ZnFeO (co-prec) & ZnFeO (sol-gel), and (c) ZnFeCoO (co-prec) & ZnFeCoO (sol-gel) nanoparticles.

The different ranges of frequencies along with their respective properties are shown in Table.2. The transmittance peak that was found at a frequency of  $670\text{ cm}^{-1}$  in ZnFeCoO sample synthesized by sol gel method is due to Fe-O bond vibration [29]. The band frequencies from  $850$  to  $900\text{ cm}^{-1}$  are attributed to the bond between oxygen and cobalt. We can also observe that there are some additional peaks between  $600$  to  $1000\text{ cm}^{-1}$  which are due to ZnO and Co-O bonding which may be the possibility of some additional faces at higher concentration of iron and cobalt co-doping. Transmittance peaks observed at  $1125\text{ cm}^{-1}$  for iron doped sample synthesized by co precipitation and sol gel sample are due to C–O stretching vibration [30]. Weak frequency band observed between  $1300$  to  $1400\text{ cm}^{-1}$  is due to O-H bonding of water or due to typical organic group of carbon [31-33].

The variation in FTIR spectra for the samples synthesized by two different techniques can easily be observed from the Fig 2. Table shows the FTIR peaks assignments to different vibrational modes for all the six samples.

Table 2. FTIR peaks assignment to different vibrational modes of ZnO(co-prec), ZnO(sol-gel), ZnFeO(co-prec), ZnFeO(sol-gel), ZnFeCoO(co-prec) and ZnFeCoO(sol-gel) nanoparticles.

Assignments	Wavenumber (cm <sup>-1</sup> )					
	ZnO (co-prec)	ZnO (sol-gel)	ZnFeO (co-prec)	ZnFeO (sol-gel)	ZnFeCoO (co-prec)	ZnFeCoO (sol-gel)
Zn-O bond (tetrahedral)	369	373	370	370	370	370
Zn-O bond (octahedral)	517	519	510	510	500	670
Co-O stretching mode and ethanol precursors	No peak	No peak	638	No peak	No peak	No peak
Microstructural changes						
Asymmetric stretching of C=O bond	883	885	880	868, 880	868	864
H-O-H bending vibration	No peak	No peak	1125	1125	No peak	No peak
	1383	1382	1385	1385	1385	1386

### 3.3. Optical study

Optical spectra in the range 200 nm to 500 nm wavelength at room temperature is exhibited in Fig.3. Different parameters such as band gap, impurities, oxygen deficiency and roughness of the surface are responsible for absorbance.

UV absorption spectroscopy was used to check the impact of Fe and Co doping on optical properties of ZnO nanoparticles and also to compare the absorbance for the samples synthesized by two divergent methodologies. Strong UV absorption peaks at wavelength 409 nm are noticed for ZnO(co-prec) and 395 nm for ZnO(sol-gel) that can be created from the recombination of localized level excited electrons below the conduction band with the holes in valence band. The iron doped sample have absorption peaks at 359 nm for co precipitation sample and 344 nm for sol gel sample as mentioned in the Fig.3.

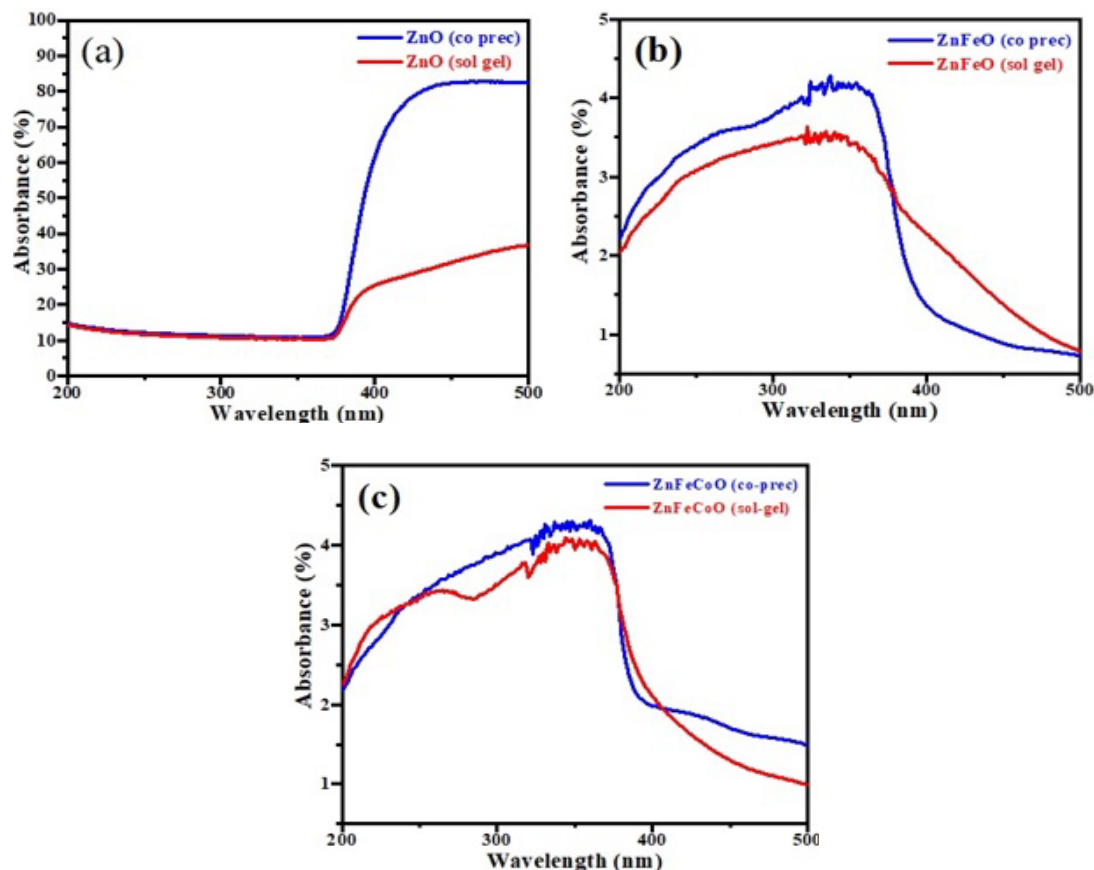


Fig. 3. UV-Visible absorption spectra of (a) ZnO (co-prec) & ZnO (sol-gel) (b) ZnFeO (co-prec) & ZnFeO (sol-gel), and (c) ZnFeCoO (co-prec) & ZnFeCoO (sol-gel) nanoparticles.

The absorption peaks for iron and cobalt co-doped sample were observed at 337 nm for co precipitation sample and 322 nm for sol gel sample as mentioned. The minor shift of the absorption peak for different synthesis technique may be originated because of variation of particle size and their arrangement [34]. The observed absorption peaks are shifted towards the shorter wavelength due to cobalt concentration. It can be noted that the absorption peaks are shifted with transition metal doping is due to the sp-d spin exchange interaction between electrons of host material and localized d-electrons of dopant ions [35,36]. So it may results in rise to a positive and negative shift to the valence and conduction band edges which results a wider band gap. The Burstein – Moss effect explains the blue shift in the UV absorption peak [37], according to this, by increasing carrier concentration, the Fermi level merges into conduction band, as a consequence of which the apparent band gap enhances and the absorption edge is propelled towards higher energies.

Absorbance is entirely relying on different factors such as imperfections in grain structure, size of particles and insufficiency in oxygen. Observed increase in value of ' $E_g$ ' as shown in Table.3 with doping of transition metal ion and co-doping is may be due to Co and Fe incorporating at substitutional or/and interstitial site of wurtzite structure of ZnO [38].

Table 3. Shows the band gap energy for all the samples for respective absorption peaks.

Samples	Absorption peak	Energy Band Gap
	$\lambda$ (nm)	$E_g$ (eV)
ZnO (co-prec)	409	3.03
ZnO (sol – gel)	395	3.13
ZnFeO (co-prec)	359	3.46
ZnFeO (sol-gel)	344	3.61
ZnFeCoO (co-prec)	337	3.68
ZnFeCoO (sol-gel)	322	3.86

### 3.4. Magnetic properties

Magnetic aspects were investigated by vibrating sample magnetometer (VSM) at room temperature. Synthesis technique, doping element and annealing temperature determines the magnetic properties of DMS materials. Magnetic investigation proved that, at room temperature, undoped ZnO is diamagnetic. Potzger et.al indicated that it remains diamagnetic over magnetization reversal, even at lower temperature (5 K) [39].

The relation between the magnetization ‘M’ and applied field H i.e. (M-H) curve of all the six samples ZnO, ZnFeO and ZnFeCoO annealed at 300 K synthesized by both, co precipitation and sol gel method is shown in Fig.4. Pure ZnO samples exhibited diamagnetic behavior for both synthesis techniques which is its intrinsic behavior [40]. The sample ZnFeO synthesized by both co precipitation and sol gel techniques shows hysteresis and exhibits weak room temperature ferromagnetism (RTFM). In previous researches, it was observed that the RTFM was attributed to secondary phases of dopant ions and it may also result of some type of exchange interaction [41]. In our work, as the secondary phases are absent, so it is concluded that RTFM behavior is result of some type of exchange interaction. The saturation magnetization for ZnFeO, synthesized by co-precipitation and sol gel method, was observed at 0.34 emu/g and 0.21 emu/g respectively. The saturation magnetization was increased in the same sample prepared by co precipitation method. An increment in the value of saturation magnetization for co precipitation method may be attributed to the phenomenon of washing the sample several times with water and ethanol. This slight change in value of saturation magnetization favors co precipitation method rather than sol gel method. The retentivity of the sample ZnFeO for co precipitation was 0.001 emu/g and for sol gel method it was 0.0025 emu/g. The observed values of coercivity for ZnFeO sample synthesized by co precipitation was 27 Oe and for sol gel sample it was 24 Oe. Not much difference was found in the values of coercivity for both the samples made by co precipitation and sol gel method. The low value of coercivity shows that the prepared sample is a soft ferromagnetic material.

For ZnFeCoO sample prepared by both co precipitation method and sol gel method also shows some hysteresis behavior which also exhibit weak RTFM. The observed value of saturation magnetization was 0.128 emu/g for co precipitation sample and it was 0.078 emu/g for the sample prepared by sol gel method. The retentivity of the sample ZnFeCoO prepared by co precipitation method was 0.0012 emu/g and it was 0.0061 emu/g for the sol gel method. The observed value of coercivity for ZnFeCoO sample prepared by co precipitation was 201 Oe and for sol gel sample it was 188 Oe. Small difference was observed in the values of coercivity of the same samples synthesized by co precipitation and sol gel. Hence, we deduce that magnetic saturation escalates with simultaneous doping of Fe and Co [42]. So, in this investigation, obtained ferromagnetism is an intrinsic behavior of Fe-doped and Fe–Co co-doped samples [21].

By analyzing all the doped four samples, it was concluded that RTFM was achieved to some extent and can be improved by changing the doping amount of cobalt. Also, the results favors the co-precipitation method rather than sol-gel method for enhanced magnetism.

Table 4. Magnetic properties of ZnO(co-prec), ZnO(sol-gel), ZnFeO(co-prec), ZnFeO(sol-gel), ZnFeCoO(co-prec) and ZnFeCoO(sol-gel) nanoparticles.

Sample	$M_s$ (emu/g)	$M_r$ (emu/g)	$H_c$ (Oe)
ZnFeO (co-prec)	0.34	0.001	27
ZnFeO(sol-gel)	0.21	0.0025	24
ZnFeCoO(co-prec)	0.128	0.0012	201
ZnFeCoO(sol-gel)	0.078	0.0061	188

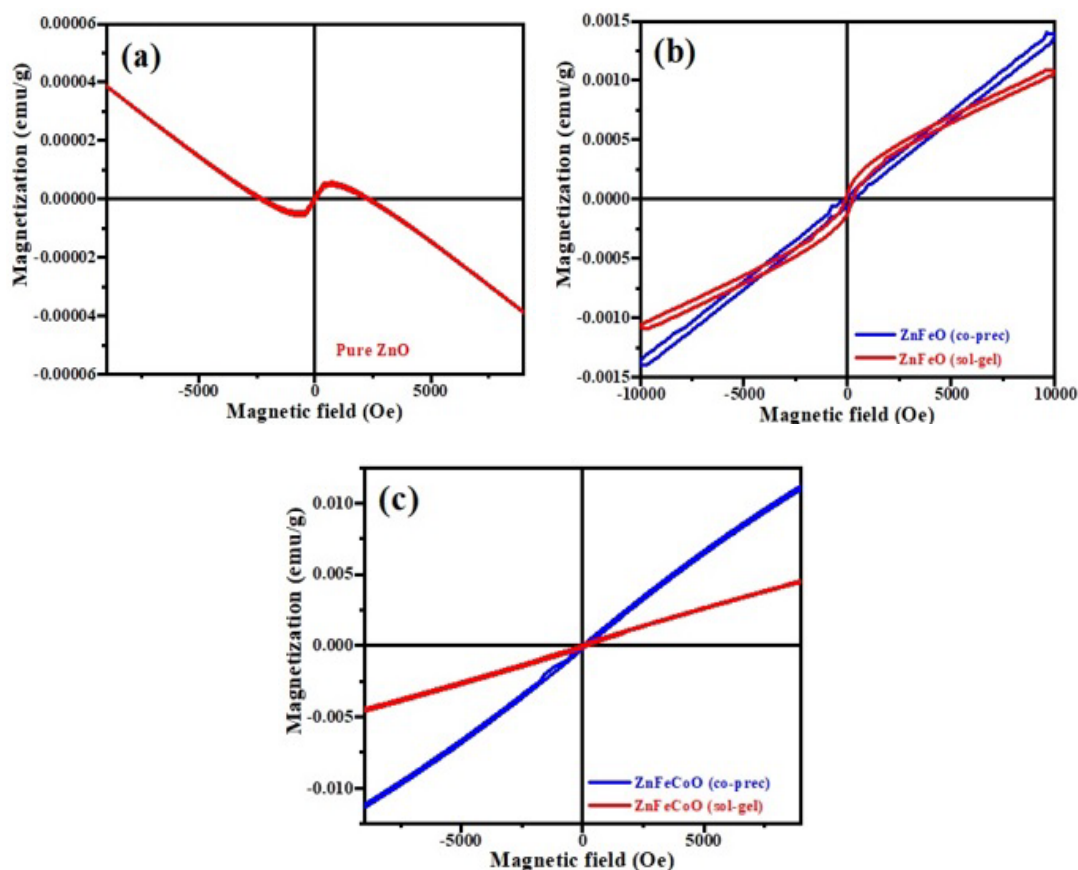


Fig. 4. M-H curves of (a) Pure ZnO (b) ZnFeO (co-prec) & ZnFeO (sol-gel), and (c) ZnFeCoO (co-prec) & ZnFeCoO (sol-gel) nanoparticles.

#### 4. Conclusion

In summary, ZnO and Co/Fe co-doped ZnO ( $Zn_{1-x}Fe_{0.05}Co_xO$ ; where  $x = 0, 0.005$ ) have been synthesized by two different procedures including sol-gel and co-precipitation techniques. Following conclusion have been made on the basis of obtained results: Synthesis method plays a crucial role in controlling phase formation, optical and magnetic responses of the nanoparticles. All the nanoparticles exhibited the hexagonal wurtzite structure with divergent microstructure. Secondary phases were completely absent in all the samples. FTIR analysis also confirms that the prepared sample have wurtzite structure.

Crystallite size varies from 18.68-37.43 nm for the samples synthesized by co-precipitation method, and it varies from 19.97-38.45 nm for sol-gel method. This difference is mainly because of several time washing of samples in co-precipitation method. Energy band gap varies from 3.03-3.68 eV for the samples prepared by co-precipitation method, and it ranges from 3.13-3.86 eV for sol-gel method. The slight shift of the absorption peak for different synthesis technique may be originated because of variation of particle size and their structural arrangement.

It is also concluded that magnetic saturation enhances with simultaneous doping of Fe and Co, as compared to only one transition metal (Fe) doping at room temperature. Weak ferromagnetic behavior was noticed for the doped nanoparticles prepared by both the techniques. The nanoparticles synthesized by co-precipitation technique exhibited high saturation magnetization and high coercivity values. The improved magnetic behavior favors the co precipitation method over sol gel method for attaining the room temperature ferromagnetism (RTFM) for practical applications of spintronics.

### Acknowledgments

The authors extend their appreciation to the Deanship of Scientific Research at King Khalid University Abha 61421, Asir, Kingdom of Saudi Arabia for funding this work through the Large Groups Project under grant number RGP.2/499/44. The authors acknowledge the Deanship of Scientific Research, Vice Presidency for Graduate Studies and Scientific Research at King Faisal University, Saudi Arabia, for financial support under the annual funding track [GRANT3856].

### References

- [1] Ozin, G. A. (1992), *Advanced Materials*, 4(10), 612-649; <https://doi.org/10.1002/adma.19920041003>
- [2] Daniel, M. C., & Astruc, D. (2004), *Chemical reviews*, 104(1), 293-346; <https://doi.org/10.1021/cr030698+>
- [3] A. Djurišić, A. M. C Ng, X. Chen, *Progress in Quantum Electronics* 34 (2010) 191-259; <https://doi.org/10.1016/j.pquantelec.2010.04.001>
- [4] J. Zhang, L. Zhang, X. Peng, X. Wang, *Appl. Phys. A: Mater. Sci. Processing* 73 (2001) 773-775; <https://doi.org/10.1007/s003390101014>
- [5] Devillers, T., Jamet, M., Barski, A., Poydenot, V., Dujardin, R., Bayle Guillemaud, P. & Tatarenko, S. (2007), *Physica status solidi (a)*, 204(1), 130-135; <https://doi.org/10.1002/pssa.200673026>
- [6] Yang, Z. A., *Appl. Phys. A* 2013,112, 241-254; <https://doi.org/10.1007/s00339-013-7658-7>
- [7] R. Bhargava, P.K. Sharma, S. Kumar, A.C. Pandey, N. Kumar, *J. Solid State Chem.* 183 (2010) 1400; <https://doi.org/10.1016/j.jssc.2010.04.014>
- [8] Z.B. Bahsi, A. Yavuz Oral, *Opt. Mater.* 29 (2007) 672-678; <https://doi.org/10.1016/j.optmat.2005.11.016>
- [9] Z. Zhang, J.B. Yi, J. Ding, L.M. Wong, H.L. Seng, S.J. Wang, J.G. Tao, G.P. Li, G.Z. Xing, T.C. Sum, C.H.A. Huan, T. Wu, *J. Phys. Chem. C* 112 (2008) 9579-9585; <https://doi.org/10.1021/jp710837h>
- [10] L.-H. Ye, A.J. Freeman, B. Delley, *Phys. Rev. B* 73 (2006) 033203-033206; <https://doi.org/10.1103/PhysRevB.73.033203>
- [11] M. Ferhat, A. Zaoui, R. Ahuja, *Appl. Phys. Lett.* 94 (2009) 142502-142504; <https://doi.org/10.1063/1.3112603>
- [12] Z. Quan, D. Li, B. Sebo, W. Liu, S. Guo, S. Xu, H. Huang, G. Fang, M. Li, X. Zhao, *Appl. Surf. Sci.* 256 (2010) 3669-3675; <https://doi.org/10.1016/j.apsusc.2010.01.005>

- [13] Synthesis of ZnO nanoparticles by two different methods & comparison of their structural, antibacterial, photocatalytic and optical properties To cite this article: Md Jahidul Haque et al 2020 Nano Express 1 010007; <https://doi.org/10.1088/2632-959X/ab7a43>
- [14] Elahe Darvishi a , Danial Kahrizi a,b , Elham Arkan.(2019), Journal of molecular Liquids; <https://doi.org/10.1016/j.molliq.2019.04.108>
- [15] Xiaojuan Wu,1,2 Zhiqiang Wei,1,2 Lingling Zhang,2 Xuan Wang,2 Hua Yang,1,2 and Jinlong Jiang, Hydrothermal Synthesis. 2014. 1-6; <https://doi.org/10.1155/2014/792102>
- [16] Hassan, M. M., Ahmed, A. S., Chaman, M., Khan, W., Naqvi, A. H., & Azam, A. (2012), Materials research bulletin, 47(12), 3952-3958; <https://doi.org/10.1016/j.materresbull.2012.08.015>
- [17] Dinesha, M. L., Jayanna, H. S., Mohanty, S., & Ravi, S. (2010), Journal of alloys and compounds, 490(1-2), 618-623; <https://doi.org/10.1016/j.jallcom.2009.10.120>
- [18] Sharma, D., & Jha, R. (2017), Ceramics International, 43(11), 8488-8496; <https://doi.org/10.1016/j.ceramint.2017.03.201>
- [19] Park, M. S., & Min, B. I. (2003), Physical Review B, 68(22), 224436; <https://doi.org/10.1103/PhysRevB.68.224436>
- [20] Robina Ashraf et al Magnetic and Structural Properties of Co doped ZnO Nanoparticles (2013) 346-352
- [21] Y. Chen, X.L. Xu, G.H. Zhang, H. Xue, S.Y. Ma, Physica B 404 (2009) 3645-3649; <https://doi.org/10.1016/j.physb.2009.06.051>
- [22] M.L. Dinesha, H.S. Jayanna, S. Mohanty, S. Ravi, J. Alloys Comp. 490 (2010) 618- 623; <https://doi.org/10.1016/j.jallcom.2009.10.120>
- [23] L.B. Duan, G.H. Rao, J. Yu, Y.C. Wang, Solid State Commun. 145 (2008) 525-528; <https://doi.org/10.1016/j.ssc.2008.01.014>
- [24] Basnet, P., Samanta, D., Inakhunbi Chanu, T., Mukherjee, J., & Chatterjee, S. (2019), SN Applied Sciences, 1(6), 633; <https://doi.org/10.1007/s42452-019-0642-x>
- [25] Sans, J. A., Sánchez-Royo, J. F., Segura, A., Tobias, G., & Canadell, E. (2009). Physical Review B, 79(19), 195105; <https://doi.org/10.1103/PhysRevB.79.195105>
- [26] M. Ashokkumar, S. Muthukumaran, J. Alloys Compd. 587 (2014) 606-612; <https://doi.org/10.1016/j.jallcom.2013.10.246>
- [27] K. Vanheusden, W.L. Warren, C.H. Seager, D.R. Tallant, J.A. Voigt, B.E. Gnade, J. Appl. Phys. 79 (1996) 7983-7985; <https://doi.org/10.1063/1.362349>
- [28] Guo, Y., Cao, X., Lan, X., Zhao, C., Xue, X., & Song, Y. (2008), The Journal of Physical Chemist C, 112(24), 8832-8838; <https://doi.org/10.1021/jp800106v>
- [29] Kumar, B., Smita, K., Cumbal, L., & Debut, A. (2014), Journal of Saudi Chemical Society, 18(4), 364-369; <https://doi.org/10.1016/j.jscs.2014.01.003>
- [30] Du, X. W., Fu, Y. S., Sun, J., Han, X., & Liu, J. (2006). Semiconductor science and technology, 21(8),1202; <https://doi.org/10.1088/0268-1242/21/8/037>
- [31] K. Nakamoto, Infrared and Raman Spectra of Inorganic and Coordination Compounds, Parts-A and B. Wiley, New York, 1997.
- [32] A. Jagannatha Reddy, M.K. Kokila, H. Nagabhushana, R.P.S. Chakradhar, C. Shivakumara, J.L. Rao, B.M. Nagabhushana, J. Alloys Comp. 509 (2011) 5349- 5355; <https://doi.org/10.1016/j.jallcom.2011.02.043>
- [33] S. Senthilkumar, K. Rajendran, S. Banerjee, T.K. Chini, V. Sengodan, Mater. Sci. Semi. Proc. 11 (2008) 6-12; <https://doi.org/10.1016/j.mssp.2008.04.005>
- [34] Djurišić, A.B.; Ng, A.M.C.; Chen, X.Y., Prog.Quantum Electron. 2010, 34,191-259; <https://doi.org/10.1016/j.pquantelec.2010.04.001>
- [35] Ahmed, F., Kumar, S., Arshi, N., Anwar, M. S., & Koo, B. H. (2012). CrystEngComm, 14(11), 4016 4026; <https://doi.org/10.1039/c2ce25227a>
- [36] Chen, Z. C., Zhuge, L. J., Wu, X. M., & Meng, Y. D. (2007), Thin Solid Films, 515(13), 5462 5465; <https://doi.org/10.1016/j.tsf.2007.01.015>

- [37] A. V. Dijken, E. A. Meulenkamp, D. Vanmaelbergh, A. Meijerink, J. Phys. Chem. B 104 (2000) 1715-1723; <https://doi.org/10.1021/jp993327z>
- [38] Singh, R. P. P., Hudiara, I. S., Panday, S., & Rana, S. B. (2016), Journal of Superconductivity and Novel Magnetism, 29(3), 819827; <https://doi.org/10.1007/s10948-015-3349-2>
- [39] K. Potzger, Shengqiang Zhou, F. Eichhorn, M. Helm, W. Skorupa, A. Mücklich, J. Fassbender, J. Appl. Phys., 99 (2006) 063906; <https://doi.org/10.1063/1.2183350>
- [40] Zhou, S., Potzger, K., Reuther, H., Kuepper, K., Skorupa, W., Helm, M., Fassbender, J.: J. Appl. Phys. 101, 09H109 (2007); <https://doi.org/10.1063/1.2710802>
- [41] Sharma, V.K., Varma, G.D., Adv. Mat. Lett. (2012); <https://doi.org/10.5185/amlett.2011.7283>
- [42] Rana, S.B., Bhardwaj, V.K., Singh, S., Singh, A., Kaur, N.: Influence of surface modification by 2-aminothiophenol on optoelectronics properties of ZnO nanoparticles. J. Exp. Nanosci. 9(9), 877-891 (2014). <https://doi.org/10.1080/17458080.2012.736640>